

Advanced Solid State Detector Technologies for Particle Detection

D. Moraes¹, M. Despeisse¹, S. Dunand², P. Jarron¹, K.M. Johansen¹,

J. Kaplon¹, C. Miazza², A. Shah², N. Wyrsh²

¹ CERN, 1211 Geneva 23, Switzerland

² IMT, Rue A.-L. Breguet 2, CH-2000 Neuchatel, Switzerland

corresponding author: Danielle.Moraes@cern.ch

Abstract

Preliminary experimental results obtained with hydrogenated amorphous silicon (a-Si:H) films are presented. This material has been selected for its unique capability to be deposited on top of integrated circuits and for its excellent radiation hardness. Particle sensors using vertical integration technology were produced. The Macropixel sensor showed a noise of $41e^-$ r.m.s. at a peaking time of 160ns. Results on dark current, irradiation and direct detection of charged particles are reported.

I. INTRODUCTION

In this work we investigated a novel solid state detector technology based on the deposition of a hydrogenated amorphous silicon (a-Si:H) film on top of an ASIC, providing sensor segmentation and processing sensor signals. This approach is especially attractive for radiation hard pixel detector with pixel size ranging from $25\mu\text{m}$ to $500\mu\text{m}$ in offering a good potential for low cost and high level of radiation hardness. The vertical integration of a thin film sensor on ASIC eliminates the need of bump bonding and enables a level of integration comparable to monolithic pixel while having the advantages of the hybrid pixel approach.

The a-Si:H characteristics were first studied on test devices, where n-i-p diodes are evaporated on chromium coated glass and the pixel areas are defined by a patterned Zinc Oxide (ZnO) or Indium Tin Oxide (ITO) top electrode. The patterning is done by a rubber stamping process followed by a wet etch of the transparent conductive oxide. These structures are characterised by measuring current versus voltage (in the dark and under illumination) and transient charge collection (time of flight). The results of the characterisation are described in [1]. Results from irradiation tests with a $30\mu\text{m}$ thick test device are discussed in section V.

After the optimisation of n-i-p diodes on glass substrates, these structures have been deposited on ASICs. Some studies of charge collection efficiency under very weak pulsed light illumination and with a beta sources for two different integrated circuits are presented in references [2] and [3]. In

the present work we describe the Macropixel sensor and discuss the results obtained with a $15\mu\text{m}$ thick a-Si: film.

II. HYDROGENATED AMORPHOUS SILICON

Amorphous silicon (a:Si) is a semiconductor with silicon atoms not arranged in an ordered lattice structure as crystalline silicon. The relative position of atoms in a crystal is ordered to large pair distances, while the amorphous has short range order but lacks the long range order. This lack of structure results in coordination defects such as dangling bonds and distorted Si-Si bonds in both lengths and angles, which originates energy levels in the forbidden energy gap where electrons and holes recombine. When amorphous silicon is deposited under hydrogenation conditions, the hydrogen atoms saturate dangling and weak bonds reducing traps and increasing the tolerance to impurities. Some hydrogenated amorphous silicon (a-Si:H) properties are summarized in table 1.

Hydrogenated amorphous silicon has much lower electron and hole mobilities than crystalline silicon, but it has the advantage of being produced at low cost in large area depositions. In addition, it has the unique property of being deposited at low temperature ($<250^\circ\text{C}$) and it has been proven to be a radiation hard material [4].

Table 1: Properties of a-Si H in comparison to crystal silicon (c-Si).

Property	c-Si	a-Si:H
Hydrogen Content	0	~10-20%
Optical Band Gap at 300 K (eV)	1.12	1.7-1.8
Density (g/cm^3)	2.33	2.15-2.25
Pair creation energy (eV)	3.6	~ 3.6-5
Electron Mobility ($\text{cm}^2\text{s}^{-1}\text{V}^{-1}$)	1450	> 10
Hole Mobility ($\text{cm}^2\text{s}^{-1}\text{V}^{-1}$)	450	> 1
Full Depletion Field ($\text{V}/\mu\text{m}$)	< 1	~ 10

Its useful electrical properties were first reported by Spear and Leomber in 1976 [5]. Since then there has been considerable research and development of this material [6-10]

leading to a variety of applications such as photovoltaic panels, thin film light emitting diodes, photosensors and thin film transistors.

III. MACROPIXEL SENSOR

The Macropixel sensor, shown in Figure 1, consists of a film of a-Si:H deposited directly on top of an integrated circuit. The sensor presented here is an a-Si:H n-i-p diode with a thickness of $15\mu\text{m}$. The a-Si:H is deposited using the Very High Frequency Plasma Enhanced Chemical Vapour Deposition (VHF-PECVD) technique. The VHF is crucial for achieving high deposition rates with minimal mechanical and low defect density. The deposition is performed at a rate of $15.6\text{\AA}/\text{s}$ and a frequency of 70MHz , using hydrogen dilution of silane. The relatively low temperature of this process (between 180°C and 220°C) is compatible with post processing on finished electronic wafers.

The a-Si:H film consists of three layers: a top p-doped layer, an intrinsic sensitive layer and a bottom n-doped layer. The bottom layer is a thin ($\sim 20\text{nm}$) low conductive layer that provides pixel isolation and avoids additional patterning of the ASIC. An Indium Tin Oxide (ITO) electrode, deposited by thermal evaporation, is used as top contact.

A. Integrated Circuit

The circuit is a $4\text{x}4\text{mm}^2$ ASIC implemented in $0.25\mu\text{m}$ technology, powered with -2.5V power supply. It consists of 48 octagonal pads with about $140\mu\text{m}$ width and $380\mu\text{m}$ pitch, as shown in Figure 1. Each pad is connected to a charge amplifier with active feedback followed by a shaper stage providing CR-RC shaping. This architecture enables very high equivalent resistance of the amplifier, which is crucial for optimisation of the noise performance.

The charge sensitive amplifier has a decay time constant that produces a slight undershoot of the output signals. This undershoot doesn't influence the noise performance of the circuit. The nominal bias current for the input transistor is ranging between $200\mu\text{A}$ and $400\mu\text{A}$. The amplifier is optimised to work with a feedback current of 100pA and a detector leakage current of 10pA . For leakage currents above the nominal value the bias of the feedback transistor can be increased up to 1mA , with the penalty of increasing the parallel noise and the signal undershoot.

The shaper comprises two cascaded stages of amplifiers working in common source configuration based on PMOS and NMOS devices. The stages integrate signal with 100ns time constant. An additional low-pass filter provides attenuation of high frequency components, which are not efficiently filtered by the main shaper stage, without influencing the pulse gain of the full chain. The circuit functionality can be tested issuing calibration pulses via a 5fF internal capacitor connected to each channel input.

The Macropixel circuit has a measured gain of $430\text{mV}/\text{fC}$ and a peaking time of about 160ns . The equivalent noise charge was measured to be between $20e^-$ and $27e^-$ for feedback current varying from 30pA to 220pA . Figure 2

shows the response of two randomly selected channels (not loaded) to 0.1fC ($625e^-$) charge injected through a test capacitor. Although the circuit has been optimised for the negative input charges it can work with positive signals in a limited dynamic range.

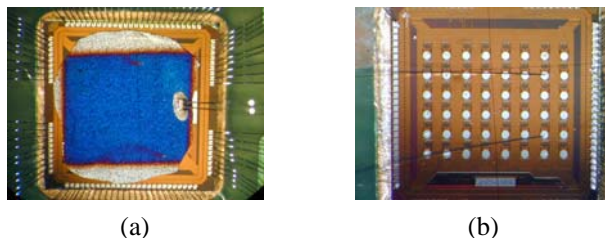


Figure 1: Photography of a Macropixel sensor (a) and integrated circuit (b). The sensor consists of an a-Si:H diode deposited on top of the ASIC. The pixels are in an array of $8\text{x}6$, with a pitch of $380\mu\text{m}$.

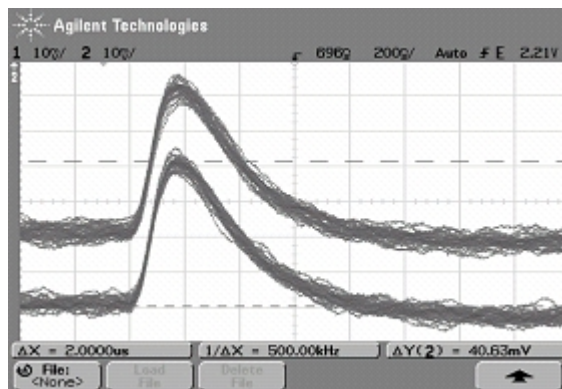


Figure 2: Response of two randomly selected channels (not loaded) of the Macropixel ASIC to 0.1fC charge injected through a test capacitor. The bias current of the input transistor is set to $300\mu\text{A}$ and the feedback current to 100pA .

IV. SENSOR PERFORMANCE

The sensor consists of a $15\mu\text{m}$ thick a-Si:H film deposited on top of the Macropixel ASIC. The negative bias voltage is applied to the top contact (ITO layer), depleting the n-i-p diode and increasing the depleted layer from the p-i interface down towards the i-n interface. The charge deposited is drifted by the electric field in the depleted layer inducing a signal on the pads connected to the amplifier. Figure 3 shows a cross section of the sensor.

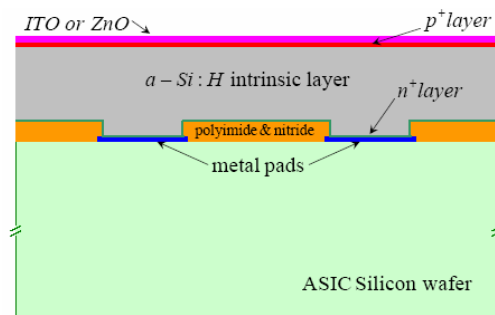


Figure 3: Cross section of an a-Si:H sensor.

1) Dark current

Figure 4 shows the sensor leakage current measured as a function of the applied electric field. The leakage current is directly measured from the biasing circuit. For a field of about $10\text{V}/\mu\text{m}$, that is close the full depletion field, the leakage current is measured to be 700pA . This value is larger than the expected values from test samples and is mainly due to the non flatness of the ASIC surface, introduced by the passivation and metal layers.

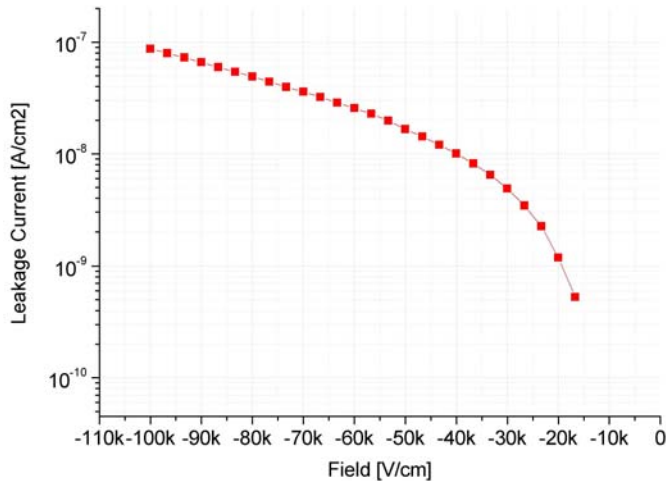


Figure 4: Leakage current as a function of the applied field measured on a $15\mu\text{m}$ sensor.

2) Noise Measurement

Figure 5 shows the noise distribution at a reverse bias of 145V and a feedback current of 800pA . A feedback current larger than the nominal value has to be applied to compensate the increase of the sensor leakage current. An equivalent noise charge of 41.5e^- r.m.s. is measured. This measurement is performed using a digital oscilloscope. The noise is in good agreement with calculations.

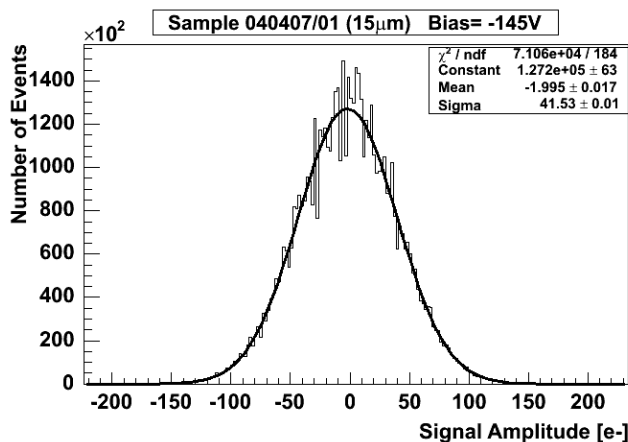


Figure 5: Equivalent noise charge measured in a $15\mu\text{m}$ sensor with a reverse bias of 145V and a feedback current equal to 800pA .

3) Particle Detection

Direct detection of charged particles is achieved in self trigger mode with the source placed directly on top of the sensor at a distance of approximately 5mm . The trigger level is set at about five sigma above the noise level. The signal from the sensor is read out by an oscilloscope connected to a LabView program. The program measures and stores the signal pedestal and amplitude.

Figure 6 shows the spectra obtained with 5.9keV energy peak from an iron source (^{55}Fe), with a reverse bias voltage of 145V . A peak at about 640e^- was measured. For crystal silicon the expected signal from this source is about 1600e^- . Assuming that the pair creation energy for a-Si:H is approximately 4eV and that only a maximum of 30% of the holes produced are collected at 160ns , due to their slow mobility, a signal of 958e^- is expected. This simple calculation suggests that the collected charge is not complete either because the diode is not fully depleted or because of possible loss of signal due to charge recombination.

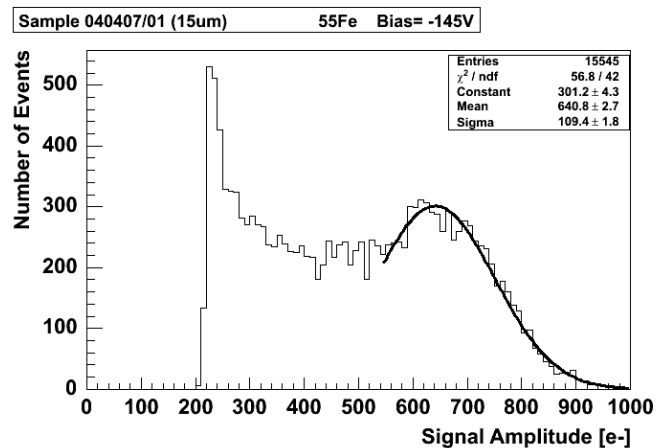


Figure 6: Spectrum of 5.9keV electrons from ^{55}Fe source, with a reverse bias voltage equal to 145V and a threshold of 200e^- .

V. IRRADIATION TESTS

A test structure with $30\mu\text{m}$ thick n-i-p a-Si:H diodes deposited on chromium coated glass is used for irradiation tests. The diodes are squares of 4mm^2 area, constantly biased at a reverse bias of 300V for full depletion. The test is performed at CERN on the IRRAD1 facility¹, which has a beam line of 24GeV protons with fluence up to $3 \times 10^{13} \text{h}^{-1} \text{cm}^{-2}$.

The accumulated dose during the irradiation was $3.5 \times 10^{15} \text{protons/cm}^2$ during 3 days. Figure 7 shows the current versus the number of spills obtained during irradiation. The “in beam” and “between beam” current is the current induced by the protons and the dark current, respectively. For reference the accumulated dose is indicated along the x-axis as yellow markers. The markers corresponds to doses of 5.9×10^{13} , 1.55×10^{15} and $3.52 \times 10^{15} \text{protons/cm}^2$, from the left to the right

¹ <http://irradiation.web.cern.ch/irradiation/irrad1.htm>

For doses up to 1.5×10^{15} protons/cm² the current drops from about $8 \mu\text{A}$ down to approximately $4 \mu\text{A}$. For higher doses it stabilizes around $2 \mu\text{A}$. A possible explanation for the drop in the current is radiation induced creation of dangling bonds. Since the dangling bonds work as recombination centres for electron hole pairs this effectively reduces the radiation induced current in the detector. The stabilization can be explained by annealing effect that compensates radiation induced dangling bonds.

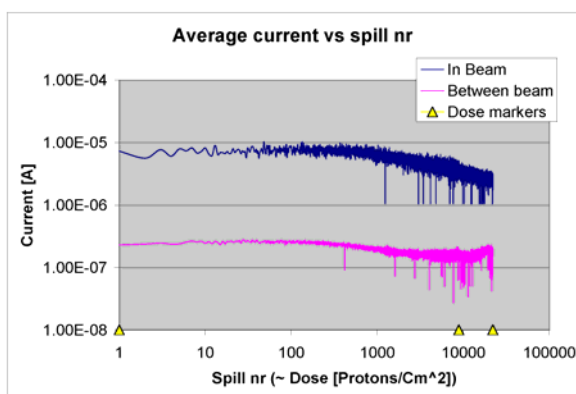


Figure 7: Measured current as a function of the increasing radiation dose on a $30 \mu\text{m}$ n-i-p diode of 4mm^2 . The top curve shows the proton induced current and the bottom one the total leakage current. The dose markers corresponds to doses of 5.9×10^{13} , 1.55×10^{15} and 3.52×10^{15} protons/cm², from the left to the right.

VI. CONCLUSION

A Macropixel sensor based on the deposition of a $15 \mu\text{m}$ a-Si:H film on top of the ASIC was developed. The deposition was performed via VHF-PCVD. The sensor shows a very low noise of about $41e^-$. Measurements with charged particles from iron source (^{55}Fe) shows that there is no full charge collection at a field of $10 \text{V}/\mu\text{m}$.

A test device $30 \mu\text{m}$ thick evaporated on chromium coated glass was used for irradiation tests. The a-Si:H film was irradiated during three days with a total accumulated dose of 3×10^{15} protons/cm². The device shows a reduction on the current induced by charged particles, but there is not considerable increase of the leakage current.

Electrical properties of hydrogenated amorphous silicon materials are being investigated. Initial studies on a-Si:H pixel sensors seem very promising but further developments are required to understand the charge collection and radiation hardness of thick a-Si:H films.

VII. ACKNOWLEDGMENTS

The authors would like to express thanks to Maurice Glaser and Federico Ravotti for their important help and contributions on the radiation tests.

VIII. REFERENCES

- [1] N. Wyrsh, S. Dunand, C. Miazza, A. Shah, G. Anelli, M. Despeisse, A. Garrigos, P. Jarron, J. Kaplon, D. Moraes, S. C. Commichau, G. Dissertori, G. M. Viertel, Phys. Stat. Sol. C1 (2004) 1284.
- [2] D. Moraes, G. Anelli, M. Despeisse, G. Dissertori, A. Garrigos, P. Jarron, J. Kaplon, C. Miazza, A. Shah, G. M. Viertel, N. Wyrsh, Journal of Non-Crystalline Solids 338-340 (2004) 729-731.
- [3] P. Jarron, G. Anelli, S. C. Commichau, M. Despeisse, G. Dissertori, C. Miazza, D. Moraes, A. Shah, G. M. Viertel, N. Wyrsh, Nucl. Inst. Meth. A518 (2004), 366 and Nucl. Inst. Meth. A518 (2004), 357.
- [4] J. Kuendig et al., Solar Energy Materials & Solar Cells 79 (2003) 425.
- [5] W.E. Spear and P.G. LeComber, Philosophical Magazine 33 (1976) 935-949.
- [6] R.A. Street, "Hydrogenated Amorphous Silicon", Cambridge University Press, 1991, ISBN0521371562.
- [7] J. Kanichi, "Amorphous and Microcrystalline Semiconductors Devices: Optoelectronic Devices", Artech House, 1991, ISBN 0-89006-490-3.
- [8] V. Pérez-Méndez, G. Cho, J. Drewery, T. Jing, S.N. Kaplan, S. Qureshi, D. Wildermuth, I. Fujieda & R.A. Street, Journal of Non-Crystalline Solids 137 (1991) 1291-1296.
- [9] R.A. Street, X.D. Wu, R. Weisfield, S. Ready, R. Apte, M. Nguyen & P. Nylen, Proc. 9th Workshop on room-temperature semiconductors, X- and γ -ray detectors, Grenoble 18-22 Sept. (1995).
- [10] J.L. Crowley, Solid State Technology, February (1992) 94-97.